

FAST TIME RESPONSE ELECTROMAGNETIC DISRUPTION MITIGATION CONCEPT

TECHNICAL NOTE

R. RAMAN,^{a*} T. R. JARBOE,^a J. E. MENARD,^b S. P. GERHARDT,^b M. ONO,^b
L. BAYLOR,^c and W.-S. LAY^a

^aUniversity of Washington, William E. Boeing Department of Aeronautics and Astronautics
Seattle, Washington

^bPrinceton Plasma Physics Laboratory, Princeton, New Jersey

^cOak Ridge National Laboratory, Oak Ridge, Tennessee

Received November 19, 2014

Accepted for Publication July 17, 2015

<http://dx.doi.org/10.13182/FST14-916>

An important and urgent issue for ITER is predicting and controlling disruptions. Tokamaks and spherical tokamaks have the potential to disrupt. Methods to rapidly quench the discharge after an impending disruption is detected are essential to protect the vessel and internal components. The warning time for the onset of some disruptions in tokamaks could be <10 ms, which poses stringent requirements on the disruption mitigation system for reactor systems. In this proposed method, a cylindrical boron nitride projectile containing a radiative payload composed of boron, boron nitride, or beryllium particulate matter and weighing ~15 g is accelerated to velocities on the order of 1 to 2 km/s in <2 ms in a linear rail gun accelerator. A partially fragmented capsule is

then injected into the tokamak discharge in the 3- to 6-ms timescale, where the radiative payload is dispersed. The device referred to as an electromagnetic particle injector has the potential to meet the short warning timescales for which a reactor disruption mitigation system must be built. The system is fully electromagnetic, with no mechanical moving parts, which ensures high reliability after a period of long standby.

KEYWORDS: electromagnetic particle injector, disruption, mitigation

Note: Some figures in this technical note may be in color only in the electronic version.

I. INTRODUCTION

Safe and reliable operation of the ITER device will require systems for safely terminating the plasma discharge after the detection of an impending disruption. A primary technology planned for use in the disruption mitigation system (DMS) is massive gas injection (MGI). The present understanding of disruption mitigation using massive gas jets is based on work conducted on several tokamaks, including DIII-D, Alcator C-MOD, ASDEX-U, JET, and other large tokamaks and is summarized in Refs. 1 through 5.

The objectives of a DMS are to minimize the damage to the tokamak vessel resulting from these three effects that result from a tokamak plasma disruption:

1. reducing thermal loads on the divertor and first wall by radiating away much of the plasma thermal energy before the plasma discharge contacts vessel components
2. reducing electromagnetic forces associated with eddy and halo currents by reducing the magnitude of the plasma currents before the plasma contacts the vessel walls and by controlling the rate at which the plasma current decays

*E-mail: raman@aa.washington.edu

3. minimizing the effect of runaway electron conversion during the current quench phase by substantially increasing the total electron and impurity density in the decaying plasma.

Extensive work on MGI studies in numerous tokamaks has improved our understanding of the phases of the disruption evolution process and of the requirements on the DMS to minimize the negative impact of these effects. References 6, 7, and 8 describe the requirements, control strategies, and control scenarios for disruption mitigation in ITER.

I.A. Limitations of the MGI System

While the MGI technique is suitable for most disruptions, it may be unsuitable for disruptions with a short warning time of < 10 ms, which is a possibility for some disruptions.⁶ This is due to the slow thermal velocity of the heavier impurity gas molecules, which limits the time needed to travel the 4- to 6-m distances before it reaches the plasma edge.^{6,9} If the valves could be mounted directly on the vessel, such as in the rupture disk injection concept,¹⁰ it may have the required fast response time. The rupture disk system has been tested on Tore-Supra with encouraging results¹¹ and is a viable scenario that needs further evaluation, including assessment of the reliability of such pressurized components installed in close proximity to a harsh radiation environment where there is the possibility for the system to prematurely trigger during normal operation and for metal fragments from the rupture disk mechanism to fall into the reactor vessel.

During mitigated gas injection experiments, the injected impurities strongly cool the boundary plasma, near the pedestal. Progressive cooling produces an unstable current profile with evolving and growing islands. Eventually, the cooling and island growth at the $q = 2$ surface finally triggers rapid cooling of the entire plasma through convection and impurity mixing.^{12,13} The core energy is dissipated by impurity radiation, and the cold dense poorly conducting outer region results in a significant reduction of wall heating.

As well described in the paper by Leonov et al.,¹⁴ in simulations examining the impurity gas assimilation by the JET plasma, MGI gas assimilation is a complicated process, not just determined by the gas flow velocity or the proximity of the gas injector to the plasma but one that may be influenced by the plasma response itself. The most important results from Ref. 14 are briefly summarized here as they provide further motivation for considering alternate impurity injection technologies.

The simulation results show that the energy loss during MGI-initiated disruption mitigation takes place in two phases. The first is the pre-thermal quench (pre-TQ) phase that lasts from the arrival of the first gas to the onset of increased transport due to magnetohydrodynamic

activity. This is followed by the second thermal quench (TQ) phase, when most of the energy is radiated. The TQ begins after a critical fraction of impurities is assimilated during the pre-TQ phase so that when the impurity content reaches an amount sufficient for radiative energy loss to overpower joule heating, the cooling front begins to propagate inward accompanied by the plasma current contraction. The simulations further suggest that the pre-TQ duration is nearly independent of the D_2 influx and is determined primarily by the accumulation of the radiating impurity. Increasing the plenum pressure or reducing the distance between the valve and plasma largely shortens the pre-TQ phase. Understanding the details of the pre-TQ phase thus seems quite important for the design of the MGI concept for reactor systems. The DMS has to be designed such that the impurity amount accumulated during the pre-TQ stage is sufficient for re-radiation of $> 90\%$ of heat flux during the subsequent TQ phase of the disruption.^{14,15} In addition, because of the very energetic nature of the plasma edge in ITER, the injected gas must first penetrate an energetic scrape-off layer and then go past an energetic pedestal. These intense edge conditions are substantially different from those on present devices, and the situation is further exasperated by the much larger volume of the ITER plasma (about 30 times the volume of the DIII-D plasma and about 7 times the volume of the JET plasma).

I.B. Advantages of Solid Material Injection

These results would suggest that systems that can inject impurities deep into the plasma, inside the $q = 2$ surface and in amounts greater than the critical assimilation amounts suggested in these simulations, may provide much more control over the evolution of the TQ phase because impurity assimilation amounts will not be governed by the pre-TQ phase.

The shell pellet concept is the first of such proposed concepts for solid material injection.¹⁶ This has the advantage that by depositing the radiative material directly in the runaway current channel formation region, both the TQ and formation of runaway electrons could be suppressed. This is what is ideally desired from a tokamak DMS.

In the method tested thus far, to a limited extent on DIII-D, pellets composed of polystyrene shells containing diagnostic levels of radiative payload consisting of boron dust or pressurized Ar gas were injected.¹⁷ The basis of the shell pellet concept is the shell burn-through and release of dispersive payload in the plasma core. The initial tests were promising in that the pellets could be delivered to the core without significantly perturbing the plasma current channel. In order to optimize the dispersion of payload in the core, the effects of shell thickness, payload material, and pellet velocity need to be understood. In addition, the shell pellet material as well as the payload should consist of boron, beryllium, or boron

nitride to be compatible with ITER requirements.¹⁸ Other solid materials such as carbon are not allowed in ITER as they react with tritium.

Another method that may overcome some of the limitations of the MGI concept is the shattered pellet¹⁹ concept. This technique consists of the injection of a large cylindrical cryogenic pellet (~15-mm diameter and ~20-mm length on DIII-D). Before entering the plasma, the pellet is shattered into submillimeter fragments by impacting on metal breaker plates. Shattering the pellet increases surface area (three to four times according to bench tests) and protects the first wall from possible damage by impact from an intact pellet. The method has been tested on DIII-D and may prove to be superior to MGI (Ref. 19). Materials considered for this concept are frozen pure D₂, Ne, Ar, or some combination of deuterium and Ar or Ne.

Both these concepts use light gases to propel them. For example, in tests conducted on DIII-D, high-pressure helium was used to propel the shell pellets.¹⁷ Similarly, pressurized H₂ or He is considered for the shattered pellet concept.⁹

A limitation with the use of gases for the pellet propulsion, whether they be solid refractory, shell, or cryogenic shatterable, is that the propellant gas limits the pellet velocity to ~300 to 400 m/s (Ref. 9). The electromagnetic particle injector (EPI) described in this technical note overcomes this limit by relying on an electromagnetic propulsion system for pellet acceleration. The primary advantage of the EPI concept over gas-propelled injectors is its potential to meet short-warning timescales. The system could also be located very close to the reactor vessel. The high levels of external magnetic fields that are present near the reactor vessel actually help to improve the efficiency of the system. As a result, the system has the potential to respond rapidly by injecting impurities within 3 ms after a command to inject is issued to the system. These details are described below.

II. THE EPI SYSTEM

A paper by Lukash et al., which is a numerical study of the radiative dissipation of the plasma stored energy as a result of Li and Be pellet injection,²⁰ mentions the deep impurity injection capability of an electromagnetic rail gun for disruption mitigation applications. The paper mentions that 18 g of Li, or 8 g of Be, which are low-Z elements, if injected into the core plasma may be adequate for achieving rapid TQ rates in ITER. Although encouraging, these require experimental validation and additional modeling to compare to the experimental results. However, the paper does not describe any of the details related to the feasibility of a rail gun installation on a reactor system. Specifically, aspects related to the EPI power supply requirements, layout of the physical system, methods to maintain continuous contact of the current

carrying armature with the rail gun electrodes, methods for removal of the sabot used for propelling the pellet, methods for remotely loading the EPI system as would be required in a harsh environment, or the very important beneficial impact of the external magnetic fields on injector operation are not discussed. These aspects and the advantages of the rail gun concept over other existing concepts for disruption mitigation are the subject of this technical note.

Figure 1a describes the injector operating principle.²¹ The projectile is placed between two conducting rails separated by ~1 to 2 cm. The length of the rails would be ~1 m long. The projectile is placed in front of a conducting spring, as shown in Fig. 1b. A capacitor bank is connected to the back end of the rails. Discharging the capacitor bank causes the current to flow along the rails²¹ as shown in Fig. 1a. The $J \times B$ forces resulting from the magnetic field created in the region between the rails and the current through the spring armature accelerate the projectile. Because of its simplicity and ability to accelerate projectiles to very high velocities (of >5 km/s), it is being actively developed for mass acceleration purposes. An issue that needs to be resolved for these high-duty-cycle applications is electrode erosion. However, in a DMS, because of the low duty cycle, electrode erosion is not expected to be an important issue. Furthermore, because of the relatively simple configuration, if it is positioned at a location that provides easy access, the entire injector could be removed for refurbishment, and a refurbished injector could be installed in its place.

Figure 1a shows the direction of the magnetic field generated by currents flowing along the rails. One way to increase the efficiency of the injector is to increase the magnetic flux that penetrates the region between the rails. This is because the current flowing in the spring armature and the magnetic field generates the accelerating $J \times B$

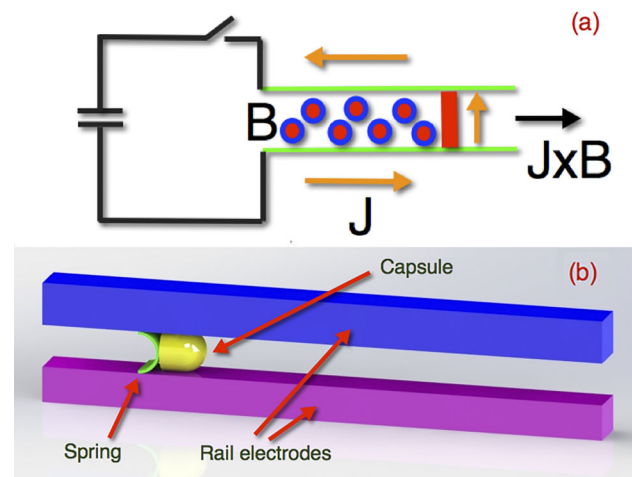


Fig. 1. (a) Rail gun operating principles and (b) electrode configuration for initial NSTX-U level test of the EPI concept.

force. To increase this field, other more complex electrode geometries are also being considered.²² However, the tokamak environment offers another potential advantage to a linear rail gun system. The ambient magnetic fields that exist near the tokamak vessel could be used to augment the gun-generated magnetic field and, as shown in Sec. III, further increase the efficiency of the injector. A typical magnetic field generated by the rail current is ~ 2 T, while the ambient magnetic field near a reactor vessel could be much larger. If the injector could be positioned sufficiently close to the vessel and the rail gun electrodes are aligned with the external magnetic field, the efficiency could be further improved. For example, the magnetic field in the ITER port plug is reported to be as high as 3 T (Ref. 6). This has the advantage that a smaller power supply and a lower level of gun current would be adequate to attain the same acceleration force. Thus, while the large ambient magnetic fields are generally an issue for most systems, it helps the linear rail gun injector improve its performance and makes the system faster acting by reducing the projectile delivery time. This is the most important advantage of the rail gun pellet delivery concept over other methods being considered for disruption mitigation applications.

III. INJECTOR PARAMETERS

The velocities that can be achieved with the EPI can be calculated by solving the rail gun equations for a linear geometry. The solution to the electrical circuit equation, which is coupled to the force equation, provides the capsule velocity and distance as a function of time.²³

For a capacitor bank with capacitance C connected to rails with inductance per unit length given as $L0$, the circuit equation is given as

$$\frac{d^2 IL}{dt^2} + R \frac{dI}{dt} + \frac{I}{C} = 0, \quad (1)$$

where

I = current through the circuit

R = total resistance composed of the external power supply resistance, cable resistance, and resistance through the load

L = total circuit inductance.

The total inductance has an external component due to the inductance of the connecting cables and the inductance of the accelerator at the location z of the projectile.

The inductance gradient is defined as the ratio of the magnetic energy per unit length of the rail to the square of the current flowing along the rails and is a measure of the amount of magnetic energy stored between the rails and can be calculated for an arbitrary electrode geometry. For

linear rails, the inductance per unit length $L0$ or the inductance gradient for square rails in which the rail separation gap is the same as the rail width can be shown to be $0.417 \mu\text{H/m}$ (Ref. 24). The total inductance L is given as

$$L(z) = L_{\text{external}} + L0 \times z. \quad (2)$$

The position z of the projectile at a given time is obtained by coupling Eq. (1) to the force equation, in which the magnetic accelerating force balances the inertia of the projectile:

$$F = m \frac{d^2 z}{dt^2} = \frac{1}{2} L0 (I^2). \quad (3)$$

The numerical solution to Eqs. (1), (2), and (3) for two different cases of an ITER-scale injector is shown in Fig. 2. These have rail dimensions of 2×2 cm, with an electrode gap of 2 cm. “ITER A” is for a capacitor bank charging voltage of 4.5 kV, and “ITER B” is for a capacitor bank voltage of 3.2 kV but with $B_T = 2$ T, the external magnetic field augmentation. For this case the contribution due to the external field IhB_T , with h being the distance between rails, should be added to the right side of Eq. (3). The injector and capsule parameters are listed in Table I.

There are a number of important observations that can be made from the simulation results. First, for a projectile mass of 15 g, a 100-mF capacitor bank charged to 4.5 kV can accelerate the capsule to ~ 1.5 km/s in ~ 1.5 ms. During this time the projectile travels ~ 1.2 m, so the injector electrode length is ~ 1.2 m for this operating scenario. Approximately 1.5 ms after the system is triggered, the capsule traveling at ~ 1.5 km/s exits the injector. If the system is located 5 m away from the plasma edge, the projectile should begin to penetrate it in ~ 7.5 ms after a command is issued to activate this DMS. Because of external magnetic field augmentation, the ITER-B case attains similar parameters but with a capacitor bank that is about half the size of the ITER-A case, as shown in Table I. Alternatively, if the original capacitor bank size is retained, a 25-g projectile would achieve similar acceleration parameters. Simulations also show that at a slightly higher operating voltage of 5.5 kV, but without external field augmentation, the projectile can reach velocities of > 2 km/s in 1.5 ms in an accelerator that is 1.7 m long.

Because of the compact nature of the injector and its simple geometry, a test of the concept could be conducted on NSTX-U or on a large tokamak. Parameters for such a device—whose primary objectives are to verify the system response time, attainable velocity parameters, and successful dispersion of the capsule payload inside the tokamak plasmas—are also shown in Fig. 2 and in Table I. Case A is for a low-power test to verify the system response time. A 20-mF capacitor bank charged to

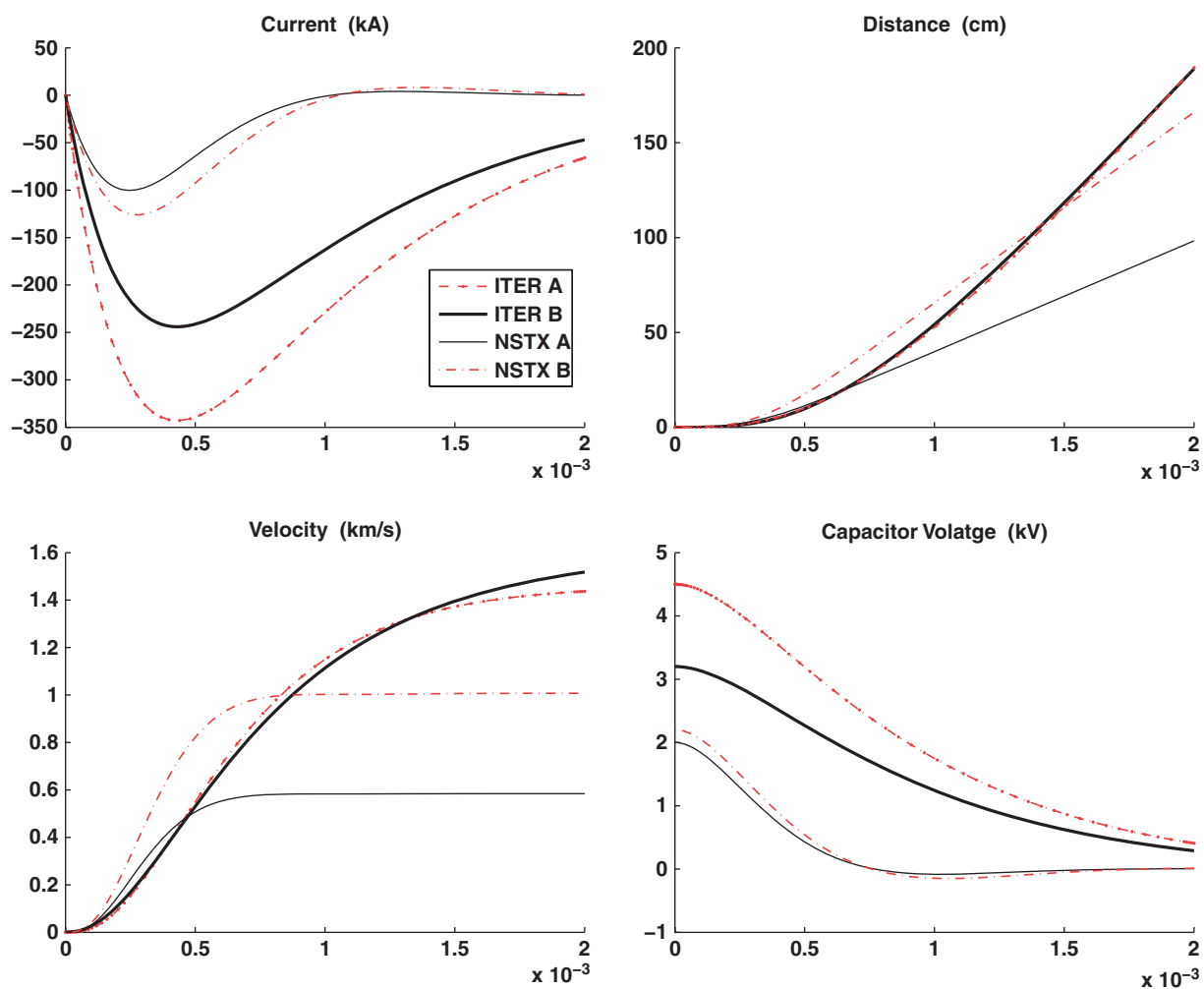


Fig. 2. Traces from simulation results showing injector current, pellet velocity, distance traveled by the projectile, and capacitor bank voltage, all as a function of time.

TABLE I

Injector and Capsule Parameters for a Reactor and NSTX-U-Scale Devices*

Injector Parameter	ITER-A	ITER-B	NSTX-A	NSTX-B
Capsule diameter (cm)	2	2	1	1
Capsule length (cm)	3.0	3.0	1.5	1.5
Capsule mass (g)	15	15	1.5	1.5
Injector length (m)	1	1.2	0.30	0.60
Bank capacitance (mF)	100	100	20	30
Bank voltage (kV)	4.5	3.2	2.0	2.2
Stored energy (kJ)	1100	510	40.0	73
Capsule velocity (km/s)	1.5	1.5	0.5	1.0
Acceleration time (ms)	1.5	1.5	0.7	1

*The present CHI capacitor bank has a stored energy of 100 kJ; the upgraded bank has a projected stored energy of 310 kJ. The ITER-B case utilizes 2-T external magnetic field augmentation.

2 kV accelerates a 1.5-g projectile to >0.5 km/s in ~ 0.7 ms in an accelerator that is 30 cm long. As the operating voltage is increased to 2.2 kV and the bank size increased to 30 mF, the velocity increases to ~ 1 km/s in 1 ms in an accelerator that is ~ 60 cm long. NSTX case A (“NSTX-A”) should be adequate for a test on NSTX-U, while NSTX case B (“NSTX-B”) would serve as in intermediate off-line test toward developing a larger-scale injector. The voltage waveform for all these cases shows that for the chosen capacitor bank size, the energy in the capacitor is depleted on the acceleration timescale. The peak acceleration currents for the four cases range from 80 kA for the low-power NSTX-U case to a maximum of ~ 350 kA for the ITER-A case.

The power supplies needed to power such an injector already exist on NSTX-U. The present coaxial helicity injection (CHI) system capacitor bank²⁵ has a capacitance of up to 50 mF and a maximum operating voltage of 2 kV. This capacitor bank will undergo a planned upgrade to increase its stored energy (to 70 mF, 3 kV, 0.3 MJ) during 2017 and could be used to support a higher-power test at $\sim 50\%$ of the ITER-scale injector. This capacitor bank would be 60% of the size of the ITER-B case and 30% of the size of the ITER-A case.

III.A. Pellet Capsule Requirements

A cylindrical shell pellet capsule would be fabricated out of thin (<0.5 mm thick) boron nitride, with a rounded front end. The cylindrical shape in combination with a rounded front end is chosen to allow the capsule to easily travel through the guide tube with a shallow bend to avoid direct streaming of neutrons back to the injector. The hollow shell pellet would be filled with boron nitride spheres, although for ITER applications, beryllium or pure boron spheres could also be considered. The simplest case would be pure radial injection, for which the capsule would be fragmented prior to injection using a shatter plate,¹⁹ or by introducing sharper bends in the guide tube itself to fracture it inside the guide tube. The capsule must be filled with particles (spheres) of proper size so that they penetrate deep into the plasma before being fully ablated.

The second possibility is to inject the capsule intact. In this case, the capsule would be injected tangentially or with a guide tube bend along the horizontal direction as shown in Fig. 3 so that in the absence of plasma, the capsule could leave the vessel through a suitably located port at end of the pellet’s trajectory. However, this is a much more difficult scenario for the following reasons. Experimentally, one needs to know the minimum shell thickness that allows the pellet to propagate through a guide tube intact. This would be a function of both the guide tube bend radius and the pellet velocity. Additionally, pellets with this wall thickness must be able to fragment inside the plasma discharge as a result of heating and pressurization of the pellet cavity due to energetic particle bombardment. For fragmented pellet injection,

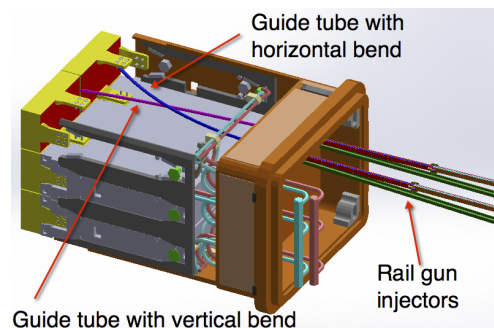


Fig. 3. Hypothetical installation configuration for the injector being located behind a midplane port plug. Shown are configurations with the pellet guide tube having a vertical bend for radial injection, and with a horizontal bend for tangential injection to allow an unfragmented pellet to exit the vessel through a suitable port at the end of the pellet trajectory. The second configuration may not be suitable for ITER but could be incorporated into the design of future devices.

only the impurity particle size (size of the spheres) inside the capsule needs to be established; this should largely be a function of the velocity of the impurity particles and the plasma parameters. Some work has been carried out for the shell pellet concept,¹⁶ but much more effort is needed to adequately establish the design for the pellet capsule and to quantify the ablation rates of differently sized impurity particles inside an ITER plasma,²⁰ with parameters that range from low-power ohmic discharges to full-power discharges. It is useful to note that the issues related to the capsule design share some commonality with the design of capsules for the shell pellet injection concept as well and is not the subject of this technical note.

IV. CONFIGURATION FOR A REACTOR

In the case of ITER, positioning the injector behind the port plug, for example as shown in Fig. 3, allows for easier maintenance, and the injector components are kept well below the bake-out temperatures to which the port plugs may be subjected. As shown in Fig. 4a, attached to the back of the electrodes would be the cartridge loading assembly. The pellet insertion tool would position a cartridge just inside the electrode region for injection. A cylindrical projectile would exit through a circular hole in the sabot removal system, as shown in Fig. 4b. The metallic spring that acts on the projectile would be captured and removed using a conveyor belt assembly that is located in the channel located below the main electrodes, as shown in Fig. 4b. A plunger system located at the side of the injector is used to remove unused capsules or capsules that have been in the injector for a prolonged period. These capsules would also drop into the conveyor belt assembly as shown in Figs. 4a and 4b. The

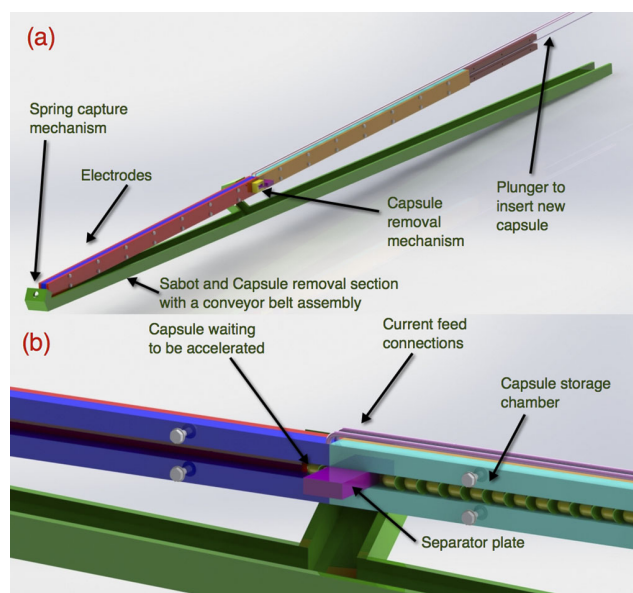


Fig. 4. (a) The entire injector assembly, including the electrodes, the spring capture mechanism, the capsule and spring removal section, and the plunger to position a new capsule and (b) a more detailed view of the capsule storage area, a capsule that is waiting to be accelerated, the separator plate that isolates the storage area from the acceleration area, and the current feed connections.

current feed lines would connect to the top of the electrode and would be kept close together to reduce their inductance. The injector would be installed in a manner so that the dominant external magnetic field is aligned with the injector-produced magnetic field to increase injector efficiency. This would result in less injector current required to achieve the same final velocity. The compact and simple nature of the injector allows the entire assembly to be easily removed for repairs and maintenance while a refurbished injector could be installed in its place.

Because the system does not rely on injecting plasmas or does not rely on plasmas for propulsion (for example, as in the plasma gun injector²⁶), the system could be positioned in a high-magnetic-field environment. A very important advantage of the EPI system is that not only is it well suited for operation in a high-magnetic-field environment, but also because it does not rely on plastic seals or cryogenic materials, it can be located close to the reactor vessel to reduce the response time for impurity particle delivery time to the tokamak. The performance improvement is twofold. First, if the system is installed near the wall, the particles could be delivered to the plasma 3 ms after the system is energized. Second, the required electrode current is reduced, which proportionally reduces the size of the power supply, as shown in Table I and in Fig. 2.

Because the ITER system is based on the use of port plugs, installing the injector inside the port plugs would limit access to the hardware. However, in future reactor devices, where something like the EPI system is incorporated into the design from an early stage, the necessary housing for the injector could be made part of the design to allow it to be positioned close to the vessel while retaining full access. The physical limitation would depend on the allowed bend in the guide tube to avoid direct streaming of neutrons back into the injector region. The injector could be mounted on rails that extend much farther out in radius so that the entire assembly could be remotely pulled out for maintenance.

An issue to be addressed is the deposition of unablated solid shell pellets on the divertor tiles. The ITER plasma-facing regions contain ~ 9.4 tonnes of Be and ~ 46 tonnes of tungsten. Discussions with ITER personnel listed in the Acknowledgement section suggest that several tens of grams of melted Be and W could get deposited on the divertor tiles as a result of localized melting resulting from unplanned events. In this case, the procedure is to use plasma discharges to ablate and disperse this material. Interestingly, on NSTX, on an occasion when several grams of localized lithium was deposited on the divertor tile, several plasma discharges with the divertor strike point intersecting these lithium deposits were used to ablate and disperse the lithium. Thus, a 15-g unablated low-Z capsule, if it were to fall on to the divertor tile, should also be removable by running plasma discharges to ablate it away by the substantially more energetic and longer-pulse ITER discharges.

V. CONCLUSIONS

An EPI based on a linear rail gun concept has the potential for rapid response and the ability to accelerate the payload capsule of ~ 15 g to 1 to 2 km/s in < 2 ms, which is adequate to meet the fast response time needed for a DMS. Increases to the size of the injector to transport a larger capsule are possible. However, a better approach is to have multiple injectors at different toroidal locations so that there is more flexibility in the amount of injected impurities, as a low-power ohmic plasma would require much less impurity injection than a full-power ITER discharge. In addition, for a full-power disruption, the ability to inject from different toroidal locations would improve impurity mixing and reduce the radiated power-peaking factors.

A very important advantage of the EPI system is that its performance substantially improves if could be installed more closely to the reactor vessel, which is possible because it does not use plastic seals, and augmentation by the external magnetic field reduces the injector current to attain the required injection velocity.

As a next step, a small prototype could be built for verification of velocity parameters. Such a system could then be tested on NSTX-U or on an existing tokamak to qualify its ability to rapidly quench a plasma discharge and to develop the experimental database on macro-particle penetration and ablation physics inside high-temperature plasma.

ACKNOWLEDGMENTS

We are grateful to M. Lehnen of the ITER Organization for providing information related to materials that are suitable for use in an ITER DMS. Many thanks to R. Feder [Princeton Plasma Physics Laboratory (PPPL)], G. Loesser (PPPL), J. Kiabacha (PPPL), L. Konkel (PPPL), V. Barabash (ITER), and M. Raphael (ITER) for providing drawings of the ITER port plug, for providing information on materials allowed in ITER, and for other help. We would like to thank E. Hollmann of the University of California, San Diego, and the DIII-D Team for providing information on the shell pellet being considered for use on DIII-D. This work is supported by U.S. Department of Energy contract numbers DE-SC0006757 and DE-AC02-09CH11466.

REFERENCES

1. E. M. HOLLMANN et al., "Measurements of Injected Impurity Assimilation During Massive Gas Injection Experiments in DIII-D," *Nucl. Fusion*, **48**, 115007 (2008); <http://dx.doi.org/10.1088/0029-5515/48/11/115007>.
2. G. M. OLYNYK et al., "Rapid Shutdown Experiments with One and Two Gas Jets on Alcator C-Mod," *Nucl. Fusion*, **53**, 092001 (2013); <http://dx.doi.org/10.1088/0029-5515/53/9/092001>.
3. G. PAUTASSO et al., "Disruption Studies in ASDEX Upgrade in View of ITER," *Plasma Phys. Control. Fusion*, **51**, 124056 (2009); <http://dx.doi.org/10.1088/0741-3335/51/12/124056>.
4. M. LEHNEN et al., "Disruption Mitigation by Massive Gas Injection in JET," *Nucl. Fusion*, **51**, 123010 (2001); <http://dx.doi.org/10.1088/0029-5515/51/12/123010>.
5. C. REUX et al., "Experimental Study of Disruption Mitigation Using Massive Injection of Noble Gases on Tore Supra," *Nucl. Fusion*, **50**, 095006 (2010); <http://dx.doi.org/10.1088/0029-5515/50/9/095006>.
6. E. M. HOLLMANN et al., "Status of Research Toward the ITER Disruption Mitigation System," *Phys. Plasmas*, **22**, 021802 (2015); <http://dx.doi.org/10.1063/1.4901251>.
7. M. LEHNEN et al., "Disruptions in ITER and Strategies for Their Control and Mitigation," *J. Nucl. Mater.*, **463**, 39 (2015); <http://dx.doi.org/10.1016/j.jnucmat.2014.10.075>.
8. M. SUGIHARA et al., "Disruption Scenarios, Their Mitigation and Operation Window in ITER," *Nucl. Fusion*, **47**, 337 (2007); <http://dx.doi.org/10.1088/0029-5515/47/4/012>.
9. L. R. BAYLOR et al., "Disruption Mitigation System Developments and Design for ITER," *Fusion Sci. Technol.*, **68**, 211 (2015); <http://dx.doi.org/10.13182/FST14-926>.
10. S. K. COMBS et al., "Alternative Techniques for Injecting Massive Quantities of Gas for Plasma-Disruption Mitigation," *IEEE Trans. Plasma Sci.*, **38**, 400 (2010); <http://dx.doi.org/10.1109/TPS.2009.2038781>.
11. F. SAINT-LAURENT et al., "FIRE, A Novel Concept of Massive Gas Injection for Disruption Mitigation in ITER: Validation on Tore Supra," *Fusion Eng. Des.*, **89**, 12, 3022 (2014); <http://dx.doi.org/10.1016/j.fusengdes.2014.09.007>.
12. V. A. IZZO, "A Numerical Investigation of the Effects of Impurity Penetration Depth on Disruption Mitigation by Massive High-Pressure Gas Jet," *Nucl. Fusion*, **46**, 541 (2006); <http://dx.doi.org/10.1088/0029-5515/46/5/006>.
13. E. M. HOLLMANN et al., "Characterization of Heat Loads from Mitigated and Unmitigated Vertical Displacement Events in DIII-D," *Phys. Plasmas*, **20**, 062501 (2013); <http://dx.doi.org/10.1063/1.4810792>.
14. V. LEONOV et al., "Simulation of the Pre-Thermal Quench Stage of Disruptions During Massive Gas Injection and Projections for ITER," *Proc. IAEA Fusion Energy 2014 Conf.*, St. Petersburg, Russia, October 13–18, 2014, International Atomic Energy Agency (2014).
15. P. B. PARKS and W. WU, "Modeling Penetration and Plasma Response of a Dense Plasma Neutral Gas Jet in a Post-Thermal Quenched Plasma," *Nucl. Fusion*, **54**, 023002 (2014); <http://dx.doi.org/10.1088/0029-5515/54/2/023002>.
16. P. B. PARKS, "Dust Ball Pellets for Disruption Mitigation," DOE Invention Disclosure, Case No. S-113-472, U.S. Department of Energy (2007).
17. E. M. HOLLMANN et al., "Low-Z Shell Pellet Experiments on DIII-D," *AIP Conf. Proc.*, **1161**, 65 (2009); <http://dx.doi.org/10.1063/1.3241211>.
18. "ITER Vacuum Handbook," IDM Ref. ITER_D_2EZ9UM (Sep. 13, 2012).
19. N. COMMAUX et al., "Demonstration of Rapid Shutdown Using Large Shattered Deuterium Pellet Injection in DIII-D," *Nucl. Fusion*, **50**, 112001 (2010); <http://dx.doi.org/10.1088/0029-5515/50/11/112001>.
20. V. E. LUKASH et al., "Modeling of Major Disruption Mitigation by Fast Injection of Massive Li Pellets in ITER Like Tokamak-Reactor," International Atomic Energy Agency (2010); <http://www-naweb.iaea.org/napc/physics/fec/fec2010/html/node191.htm#41805> (current as of Nov. 19, 2014).
21. G. C. LONG and W. F. WELDON, "Limits to the Velocity of Solid Armatures in Railguns," *IEEE Trans. Magnetics*, **25**, 1, 347 (1989); <https://dx.doi.org/10.1109/20.22562>.
22. M. S. BAYATI and A. KESHTKAR, "Study of the Current Distribution, Magnetic Field, and Inductance Gradient of Rectangular and Circular Railguns," *IEEE Trans. Plasma Sci.*, **41**, 5, 1376 (2013); <http://dx.doi.org/10.1109/TPS.2013.2251477>.
23. J. H. HAMMER et al., "Experimental Demonstration of Acceleration and Focusing of Magnetically Confined Plasma Rings," *Phys. Rev. Lett.*, **61**, 25, 2843 (1988); <https://dx.doi.org/10.1103/PhysRevLett.61.2843>.

24. A. KESHTKAR, "Effect of Rail Dimension on Current Distribution and Inductance Gradient," *IEEE Trans. Magnetics*, **41**, 1, 383 (2005); <http://dx.doi.org/10.1109/TMAG.2004.838761>.
25. R. RAMAN et al., "Non-Inductive Solenoid-Less Plasma Current Startup in NSTX Using Transient CHI," *Nucl. Fusion*, **47**, 792 (2007); <http://dx.doi.org/10.1088/0029-5515/47/8/009>.
26. I. N. BOGATU et al., "Plasma Jets for Runaway Electron Beam Suppression," *Proc. 24th IAEA Conf. Fusion Energy*, San Diego, California, October 8–13, 2012, International Atomic Energy Agency (2012).